JOC Article

Polar Hetero-Diels−Alder Reactions of 4-Alkenylthiazoles with 1,2,4-Triazoline-3,5-diones: An Experimental and Computational Study

Mateo Alajarín,*,† José Cabrera,† Aurelia Pastor,† Pilar Sánchez-Andrada,† and Delia Bautista‡

Departamento de Química Orgánica, Facultad de Química, and Servicio de Instrumentación Científica, Universidad de Murcia, Campus de Espinardo, 30100 Murcia, Spain

alajarin@um.es

Received October 5, 2007

The hetero-Diels−Alder reactions of 4-alkenylthiazoles with 4-phenyl-1,2,4-triazoline-3,5-dione (PTAD) lead to new heteropolycyclic systems in excellent yields and high levels of stereocontrol through an exclusively suprafacial approach. 4-Alkenylthiazoles with a stereogenic center placed at the alkenylic substituent react with PTAD giving the corresponding chiral cycloadducts in moderate diastereomeric excesses. The stereochemical course is dominated by the steric interactions at the two diastereomeric transition states. A computational study of these processes with structurally simpler reagents has been carried out. A concerted pathway via a highly asynchronous transition state is preferred for 2-unsubstituted 4-vinyl and 4-styrylthiazoles. However, two alternative and equally likely pathways, concerted and stepwise, have been found to be followed by 2-methyl- or 2-phenyl-substituted 4-styrylthiazoles. The concerted pathway features a highly asynchronous transition state. For the stepwise pathway, the rate-determining step is the first one, as the energy barrier for the second step is virtually nonexistent.

Introduction

The Diels−Alder reaction is one of the most versatile methods for the construction of six-membered rings, as it has been extended to a wide range of dienes and dienophiles.[1] In general, alkenyl-substituted aromatic heterocycles and their benzoderivatives undergo Diels−Alder reactions with the concourse of the diene moiety that includes the side chain double bond (extra-annular addition).[2] In most cases this way of interacting is preferred to that involving the proper heteroaromatic nucleus (intra-annular addition) as far as this nucleus contains in turn a conjugated diene arrangement.[3] Recently, we have demonstrated

† Departamento de Química Orgánica.
‡ Servicio de Instrumentación Científica.

(1) (a) Oppolzer, W. In *Comprehensive Organic Synthesis*; Trost, B. M., Fleming, I., Eds.; Pergamon Press: Oxford, UK, 1991; Vol. 5, pp 315−399. (b) Fringuelli, F.; Taticchi, A. In *The Diels−Alder Reaction−Selected Practical Methods*; Wiley: Chichester, UK, 2002. (c) Nicolaou, K. C.; Snyder, S. A.; Montagnon, T.; Vassilikogiannakis, G. *Angew. Chem., Int. Ed.* **2002**, *41*, 1668−1698.

(2) (a) Sepúlveda-Arques, J.; Abarca-González, B.; Medio-Simón, M. *Adv. Heterocycl. Chem.* **1995**, *63*, 339−401. (b) Çavdar, H.; Saraçoğlu, N. *J. Org. Chem.* **2006**, *71*, 7793−7799.

(3) (a) Jones, R. A.; Marriott, M. T. P.; Rosenthal, W. P.; Sepúlveda-Arques, J. *J. Org. Chem.* **1980**, *45*, 4515−4519. (b) Xiao, D.; Ketcha, D. M. *J. Heterocycl. Chem.* **1995**, *32*, 499−503. (c) Noland, W. E.; Wann, S. R. *J. Org. Chem.* **1979**, *44*, 4402−4410. (d) Eitel, M.; Pindur, U. *J. Org. Chem.* **1990**, *55*, 5368−5374. (e) Pindur, U.; Kim, M.-H.; Rogge, M.; Massa, W.; Molinier, M. *J. Org. Chem.* **1992**, *57*, 910−915. (f) Back, T. G.; Pandyra, A.; Wulff, J. E. *J. Org. Chem.* **2003**, *68*, 3299−3302. (g) Du, H.; He, Y.; Sivappa, R.; Lovely, C. J. *Synlett* **2006**, *7*, 965−992. (h) Dilley, A. S.; Romo, D. *Org. Lett.* **2001**, *3*, 1535−1538. (i) Dransfield, P. J.; Wang, S.; Dilley, A.; Romo, D. *Org. Lett.* **2005**, *7*, 1679−1682. (j) Marrocchi, A.; Minuti, L.; Taticchi, A.; Scheeren, H. W. *Tetrahedron* **2001**, *57*, 4959−4965. (k) Le Strat, F.; Vallete, H.; Toupet, L.; Maddaluno, J. *Eur. J. Org. Chem.* **2005**, 5296−5305. (l) Scully, J. F.; Brown, E. V. *J. Am. Chem. Soc.* **1953**, *75*, 6329−6330. (m) Moody, C. J.; Rees, C. W.; Tsoi, S. C. *J. Chem. Soc., Perkin Trans. 1* **1984**, 915−920.

10.1021/jo7021668 CCC: $40.75
Published on Web 01/04/2008

that 4-alkenylthiazoles behave as reactive all-carbon dienes in Diels−Alder reactions with the participation of the formal C−C double bond of the thiazole ring and the side chain double bond,[4] in spite of the fact that the thiazole nucleus loses its aromaticity in the reaction path and this should lead to relatively less exothermic reactions when compared to classical Diels−Alder processes.[5] Their reactions with *N*-substituted maleimides, maleic anhydride, and naphthoquinone take place with high levels of stereocontrol to give the corresponding *endo*-cycloadducts in good to excellent yields although, depending on the dienophile, the cycloadduct further transforms under the reaction conditions through either a 1,3-hydrogen shift, dehydrogenation, or an ene reaction or Michael addition with another molecule of dienophile.[4]

1,2,4-Triazoline-3,5-diones (TADs) are among the most reactive dienophiles due to their low LUMO energies.[6] Their Diels−Alder reactions are exceptionally useful in trapping unstable intermediates,[7] characterizing dienes,[8] simplifying the isolation of dienes from complex product mixtures,[9] and temporarily protecting diene moieties from reacting with chemical agents.[10] The mechanisms of both the [4+2]-cycloaddition and the ene[11] reactions with TADs have generated some controversy along the years. The main question arises from the nature of the mechanism and the implication of intermediates. For the cycloaddition processes, experimental studies indicate that both concerted and stepwise pathways may occur depending upon the diene structure.[12] Thus, for butadienes with a *s-cis* conformation readily available, the concerted pathway dominates, and the hetero-Diels−Alder products are obtained with high levels of stereocontrol. In contrast, when butadienes are highly substituted and too sterically hindered to be in the *s-cis* conformation, the stepwise mechanism becomes favored leading to poor levels of stereocontrol. To explain this lack of stereocontrol, the implication of an aziridinium imide intermediate has been suggested, although without direct experimental evidence.[12] These conclusions parallel those extracted from computational studies by using structurally simple butadienes.[13] Thus, these theoretical investigations indicated that the concerted pathway dominates with highly asynchronous transition states except for dienes that are too sterically hindered to arrange in an *s-cis* conformation.

An important feature of the Diels−Alder reaction is its potential for achieving the absolute stereochemical control of up to four contiguous centers in one step.[1] The stereochemistry of the final product results from the structure of diene and dienophile but also from their relative orientation, *endo* or *exo*, in the transition state and the *endo* approach is favored by stabilizing secondary orbital interactions.[1] However, a third stereochemical feature arises when either of the two reactants possesses two diastereotopic faces, often by virtue of containing at least one chiral center.[14] Among all the possible combinations of chiral reactants, the reactions between achiral dienes and chiral dienophiles, such as acrylates, maleates, and fumarates, have been extensively studied and are now well-established synthetic protocols.[14] In spite of the use of chiral dienes providing an alternative pathway, their use is less popular because they are prepared by more elaborated synthetic routes.[15]

Herein, we report on the hetero-Diels−Alder reactions of 4-alkenylthiazoles with 4-phenyl-1,2,4-triazoline-3,5-dione (PTAD). As expected, in these reactions 4-alkenylthiazoles behave as inner−outer dienes forming new heteropolycyclic systems in excellent yields. High levels of stereocontrol are obtained as a result of the suprafacial attack and *endo* approach of the dienophile. The facial diastereoselectivity by using chiral 4-alkenylthiazoles with a stereogenic center placed at the alkenylic substituent also has been studied, although their reactions with PTAD result in moderate diastereomeric excesses. Here we also provide an interpretation of the stereochemical biases of these cycloaddition processes. Finally, the mechanism of the reaction of some representative 4-alkenylthiazoles with 1,2,4-triazoline-3,5-dione (HTAD) has been scrutinized computationally. The results here disclosed are interesting not only from the synthetic point of view but also because they shed some light on the always controvertible mechanism of the [4+2] cycloaddition of triazolinediones with dienes.

Results and Discussion

Reactions of Achiral 4-Alkenylthiazoles 1a−d with PTAD. The reactions of 4-alkenylthiazoles **1a−d**[16] with PTAD were conducted in toluene at room temperature (Scheme 1). After 5 min the initial purple color of the solution faded totally indicating that the reaction was complete. The 5,10a-dihydrothiazolo[5,4-*c*][1,2,4]triazolo[1,2-*a*]pyridazin-7,9-diones **2a−d** were isolated by filtration as single diastereoisomers in quantitative yields (Scheme 1 and Table 1).

We have reported that the primary adducts resulting from the [4+2] cycloaddition of **1** with *N*-substituted maleimides experienced 1,3-hydrogen migration at elevated temperatures causing the rearomatization of the thiazole ring.[17] On the contrary, the thermal treatment of the cycloadduct **2a** (toluene,

(4) Alajarín, M.; Cabrera, J.; Pastor, A.; Sánchez-Andrada, P.; Bautista, D. *J. Org. Chem.* **2007**, *72*, 2097−2105.

(5) Manoharan, M.; De Proft, F.; Geerlings, P. *J. Chem. Soc., Perkin Trans. 2* **2000**, 1767−1773.

(6) (a) Moody, C. J. *Adv. Heterocycl. Chem.* **1982**, *30*, 1−45. (b) Rádl, S. *Adv. Heterocycl. Chem.* **1997**, *67*, 119−205.

(7) Anastassiou, A. G.; Yakali, E. *J. Chem. Soc., Chem. Commun.* **1972**, 92−93.

(8) (a) Askani, R.; Chesick, J. P. *Chem. Ber.* **1973**, *106*, 8−19. (b) Imagawa, T.; Sueda, N.; Kawanisi, M. *J. Chem. Soc., Chem. Commun.* **1972**, 388. (c) Kobal, V. M.; Gibson, D. T.; Davies, R. E.; Garza, A. *J. Am. Chem. Soc.* **1973**, *95*, 4420−4421.

(9) (a) Poutsma, M. L.; Ibarbia, P. A. *Tetrahedron Lett.* **1970**, *11*, 4967−4970. (b) Poutsma, M. L.; Ibarbia, P. A. *J. Am. Chem. Soc.* **1971**, *93*, 440−450.

(10) (a) Ochi, K.; Matsunaga, I.; Nagano, H.; Fukushima, M.; Shindo, M.; Kaneko, C.; Ishikawa, M.; DeLuca, H. F. *J. Chem. Soc., Perkin Trans. 1* **1979**, 165−169. (b) Bosworth, N.; Emke, A.; Midgley, J. M.; Moore, C. J.; Whalley, W. B.; Ferguson, G.; Marsh, W. C. *J. Chem. Soc., Perkin Trans. 1* **1977**, 805−809. (c) Barton, D. H. R.; Gunatilaka, A. A. L.; Nakanishi, T.; Patin, H.; Widdowson, D. A.; Worth, B. R. *J. Chem. Soc., Perkin Trans. 1* **1976**, 821−826.

(11) Vougioukalakis, G. C.; Orfanopoulos, M. *Synlett* **2005**, 713−731.

(12) (a) Jensen, F.; Foote, C. S. *J. Am. Chem. Soc.* **1987**, *109*, 6376−6385. (b) Clenan, E. L.; Earlywine, A. D. *J. Am. Chem. Soc.* **1987**, *109*, 7104−7110.

(13) (a) Chen, J. S.; Houk, K. N.; Foote, C. S. *J. Am. Chem. Soc.* **1998**, *120*, 12303−12309. (b) Singleton, D. A.; Schulmeier, B. E.; Hang, C.; Thomas, A. A.; Leung, S.-W.; Merrigan, S. R. *Tetrahedron* **2001**, *57*, 5149−5160. (c) Leach, A. G.; Houk, K. N. *Chem. Commun.* **2002**, 1243−1255.

(14) (a) Oppolzer, W. *Angew. Chem., Int. Ed. Engl.* **1984**, *23*, 876−889. (b) Maddaluno, J. *Synlett* **2006**, *41*, 2534−2547.

(15) (a) Kozmin, S. A.; Rawal, V. H. *J. Am. Chem. Soc.* **1999**, *121*, 9562−9573. (b) Janey, J. M.; Iwama, T.; Kozmin, S. A.; Rawal, V. H. *J. Org. Chem.* **2000**, *65*, 9059−9068. (c) Garner, P.; Anderson, J. T.; Turske, R. A. *Chem. Commun.* **2000**, 1579−1580. (d) Søndergaard, K.; Liang, X.; Bols, M. *Chem. Eur. J.* **2001**, *7*, 2324−2331. (e) Urabe, H.; Kusaka, K.; Suzuki, D.; Sato, F. *Tetrahedron Lett.* **2002**, *43*, 285−289. (f) Kuethe, J. T.; Brooks, C. A.; Comins, D. L. *Org. Lett.* **2003**, *5*, 321−323.

(16) The synthesis of 4-alkenylthiazoles **1a−d** has been reported previously by the authors, see ref. 4.

(17) These compounds were obtained from the reaction of dienes **1** with *N*-substituted maleimides in acetonitrile at 120 °C, see ref 4.

SCHEME 1. The Reaction of 4-Alkenylthiazoles 1a−d with PTAD Leading to Cycloadducts 2a−d (R^1 and R^2 Defined in Table 1)

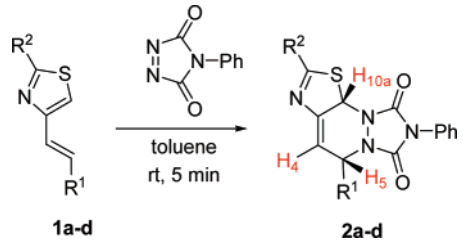

SCHEME 2. Thermal Treatment of 2a Leading to a Mixture of the Starting Thiazole 1a and 3a[a]

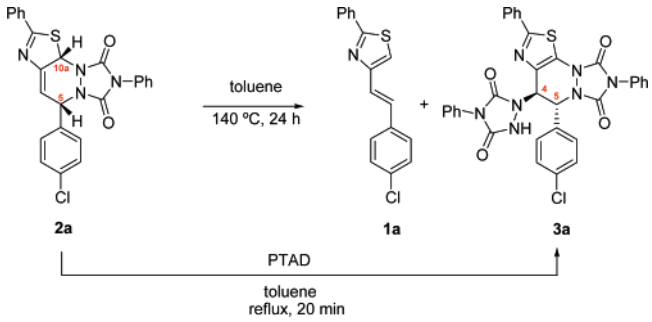

[a] The compound **3a** could be exclusively obtained by treatment of **2a** with PTAD.

SCHEME 3. Reactions of Phosphorane 5 with Chiral Aliphatic Aldehydes 6a−c and Further Synthesis of 4-Alkenylthiazoles 4a−c (R^1 and R^2 Are Defined in Table 2)

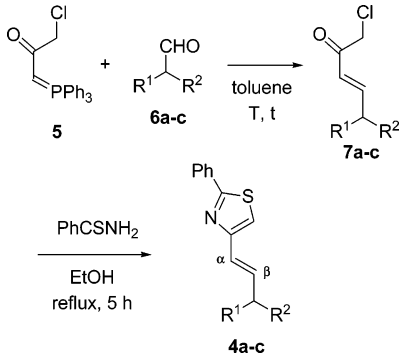

140 °C) provided a mixture of the starting diene **1a** and a new product **3a** that results from the ene reaction of **2a** with a second molecule of PTAD. Both compounds **1a** and **3a** were separated and isolated in approximately similar yields, which was 67% overall (Scheme 2). This finding may be explained taking into account the partial decomposition of **2a** into the starting materials by a retro hetero-Diels−Alder reaction and the subsequent combination of the remaining **2a** with the PTAD generated in the reaction mixture. The cycloadduct **3a** also could be prepared in nearly quantitative yield from **2a** and PTAD in refluxing toluene (Scheme 2). The ene reaction of **2a** with PTAD takes place in a highly stereocontrolled manner since **3a** was isolated as a single diastereoisomer.

The relative configurational assignment of the two stereogenic centers C_5 and C_{10a} in compounds **2** (see Scheme 1) was done by comparison of the coupling constants between their methine protons with those reported for an analogous structure.[18] These protons show mutual coupling constants in the range of 2.8−3.8 Hz, typical values for assessing a *cis* relationship between H_5 and H_{10a}.

The *trans* stereochemical relationship of compound **3a** was assigned on the basis of the X-ray structure of another 1:2 4-styrylthiazole−PTAD adduct reported below (compound **10a**) and the similarity of their NMR spectral data. In particular, the two coupling constants between their respective H_4 and H_5 protons at the six-membered ring of **3a** (see Scheme 2) present similar values (1.4 Hz). The relative configuration of **3a** reveals valuable information, i.e., the ene reaction of **2a** with PTAD is a highly stereoselective suprafacial process. This stereochemical fact was recently recognized and holds important implications for the mechanism of this type of reaction.[19]

TABLE 1. Cycloadducts 2 Resulting from the Reaction of 4-Alkenylthiazoles 1 with PTAD

thiazole	R^1	R^2	adduct	yield (%)
1a	4-ClC_6H_4	**Ph**	**2a**	quant.
1b	4-ClC_6H_4	**Me**	**2b**	quant.
1c	4-MeC_6H_4	**Ph**	**2c**	quant.
1d	4-MeC_6H_4	**Me**	**2d**	quant.

TABLE 2. Reaction Conditions and Yields in the Synthesis of α-Chloroketones 7a−c and 4-Alkenylthiazoles 4a−c

		α-chloroketones **7**				thiazoles **4**	
R1	R^2	*T* (°C)	*t* (days)	compd	yield (%)[a]	compd	yield (%)[a]
Ph	Me	rt	7	**7a**	80	**4a**	63
Ph	Et	40	5	**7b**	60	**4b**	67
$-CH_2CH_2OCH_2-$		rt	4	**7c**	75	**4c**	60

[a] After purification by column chromatography.

Study of the Facial Diastereoselectivity in the Cycloaddition Reactions of Chiral 4-Alkenylthiazoles 4a−c with PTAD. The chiral, racemic 4-alkenylthiazoles **4a−c** possess a stereogenic center directly attached to the *β*-carbon atom of the alkenylic substituent at C_4 of the thiazole ring (Scheme 3). They were easily prepared by a two-step synthetic route. Thus, (3-chloroacetonylidene)triphenylphosphorane (**5**) and the corresponding chiral aldehyde **6a−c** were reacted in toluene solution to give α-chloroketones **7a−c**. In general, these Wittig reactions were conducted in the presence of a great excess of aldehyde and at relatively low temperatures[4] to avoid polymerizations (Table 2). 4-Akenylthiazoles **4a−c** were obtained through a Hantzsch synthesis[20] from the α-chloroketones **7a−c** and thiobenzamide (Table 2).

The reaction of **4a** with PTAD in toluene at room temperature for 30 min led to a mixture of three products **8a**, **9a**, and **10a** in good overall yield (Scheme 4 and Table 3, entry 1). The two diastereoisomers **8a** and **9a** are the result of the hetero-Diels−Alder reaction of **4a** and PTAD, involving the approach of the dienophile to both diastereotopic faces of the diene, while **10a** comes from a subsequent ene reaction of one of these two diastereoisomers with a second molecule of the reagent. The three products were easily separated by chromatographic techniques. After isolation, each primary adduct, i.e., **8a** and **9a**, was reacted separately with PTAD to elucidate the origin

(18) Roa, R.; O'Shea, K. E. *Tetrahedron* **2006**, *62*, 10700−10708.

(19) Vassilikogiannakis, G.; Elemes, Y.; Orfanopoulos, M. *J. Am. Chem. Soc.* **2000**, *122*, 9540−9541.

(20) (a) Hantzsch, A. R.; Weber, J. H. *Ber. Dtsch. Chem. Ges.* **1887**, *20*, 3118−3132. (b) Schwarz, G. *Organic Syntheses*; Wiley: New York, 1955; Collect. III, pp 332 and 333.

SCHEME 4. Reactions of 4a, 8a, and 9a with PTAD

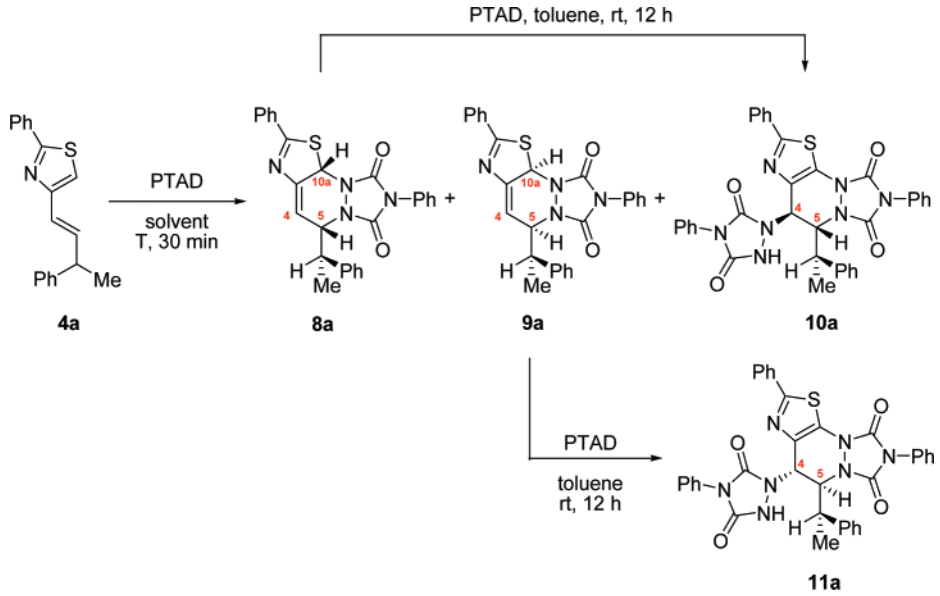

of **10a** (Scheme 4). These reactions led to **10a** from **8a**, and **11a** from **9a**, in 92% and 85% yield, respectively.

The reaction of **4a** with PTAD was also conducted at lower temperature, −5 °C, in an attempt aimed either to suppress the formation of subsequent ene adducts or/and to improve the facial diastereoselectivity of the cycloaddition step (Table 3, entry 2). After 30 min, **8a** and **9a** were exclusively isolated in 93% combined yield although in a moderate diastereomeric excess, **8a** being the major diastereoisomer. Finally, **4a** and PTAD were allowed to react in acetonitrile at −5 °C for 30 min but, under these conditions, the reaction was practically not diastereoselective (Table 3, entry 3).

The diastereoselectivity of the reactions of **4b** and **4c** with PTAD was subsequently investigated. In both cases, the hetero-Diels−Alder adducts **8b**/**9b** and **8c**/**9c** were isolated as mixtures of diastereoisomers in an approximately 63:37 ratio, **8b** and **8c** being the respective major products (Scheme 5). Although the global yields were excellent (85−90%), we were not able to resolve the diastereomeric mixtures **8b**/**9b** and **8c**/**9c** (see the Supporting Information).

The *cis* stereochemistry of the central ring of the 5,10a-dihydrothiazolo[5,4-*c*][1,2,4]triazolo[1,2-*a*]pyridazin-7,9-diones **8a**−**c** and **9a**−**c** was again evident from the coupling constants between the methine protons H_4, H_5, and H_{10a} (these positions have been marked in the structures of **8a** and **9a** in Scheme 4) with values in the range of 2.0−3.6 Hz close to those shown by cycloadducts **2**. Obviously, each pair of diastereoisomeric cycloadducts **8** and **9** results from the approximation of PTAD to both heterotopic faces of each diene **4**. The configurational assessment of **10a** was done on the basis of its

TABLE 3. Reaction Conditions and Ratio of Products 8a, 9a, and 10a Obtained in the Reaction of the Chiral 4-Alkenylthiazole 4a with PTAD

entry	solvent	*T* (°C)	**8a**:**9a**:**10a**[a]	**8a** (%)[b]	**9a** (%)[b]	**10a** (%)[b]
1	toluene	rt	43:30:27	31	24	19
2	toluene	−5	67:33:00	62	31	0
3	MeCN	−5	50:50:00	45	42	0

[a] Determined from the integration of characteristic signals in the ^{1}H NMR spectra of the crude products; error ±5% of the stated value. [b] After chromatography.

SCHEME 5. Reaction of 4-Alkenylthiazoles 4b or 4c with PTAD

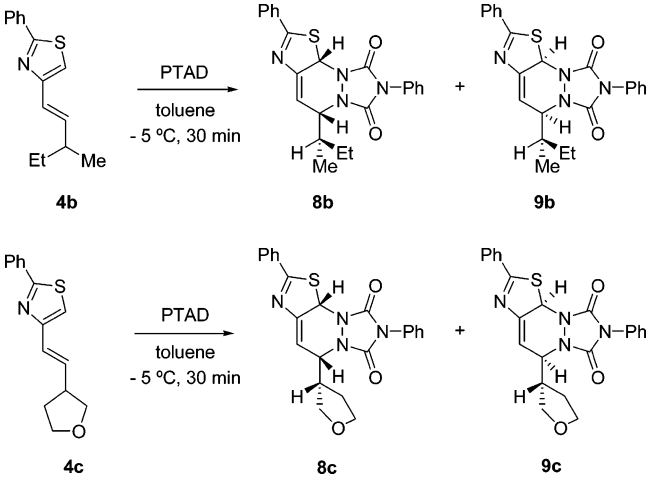

crystal structure solved by X-ray analysis (Supporting Information), which reveals a *trans* relationship between protons H_4 and H_5 and a dihedral angle between the H_4−C_4−C_5 and C_4−C_5−H_5 planes of 83°. The tridimensional architecture of **10a** in the crystals seems to be kept in solution, as the coupling constant value between these two protons, H_4 and H_5, determined from the solution ^{1}H NMR spectrum of **10a** is close to 1 Hz. The X-ray crystal structure of **10a** allowed us to assign unequivocally the relative configuration of the exocyclic stereocenter in compound **8a** and, by extrapolation, in **9a** and **11a**.

To rationalize the stereochemical course of these processes, we propose the model depicted below, which is exemplified for the particular case of the reaction of **4a** with PTAD. The vast majority of the reported examples on π-facial diastereocontrolled [4+2] cycloaddition reactions of chiral dienes involve substrates with polar functional groups placed at the allylic position.[21] Although, in general terms, the diastereofacial selectivity is directed by a subtle combination of steric and electronic effects which depend on the structure of the diene, it is usually dominated by the preference of the polar group to be in the plane of the diene and the smallest substituent at the allylic carbon, usually a hydrogen atom, as the group closest to the

SCHEME 6. The Most and Least Favorable Trajectories for the Approach of PTAD to a Single Enantiomer of 4-Alkenylthiazole 4a

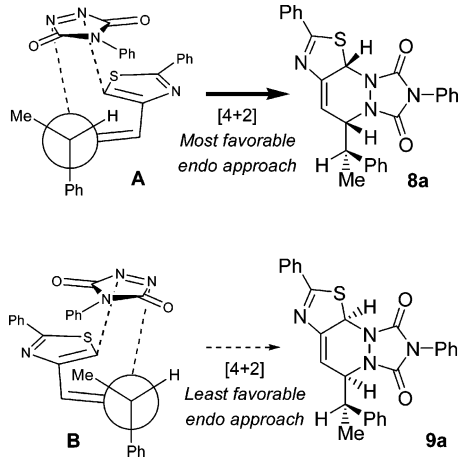

SCHEME 7. Reaction between HTAD (12) and the Thiazoles 13a−d Leading to the [4+2] Cycloadducts 14a−d

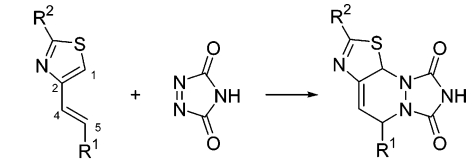

bond formation trajectory.[22] After this criterion is met the dienophile approaches from the less hindered side. On the contrary, substrates **4a**−**c** lack polar substituents and, as a consequence, this steering phenomenon. Scheme 6 shows the two alternative modes of approximating diene and dienophile, with the participation of the two diastereofaces of a single enantiomer of diene **4a**, which is depicted in its two more reasonable reactive conformations **A** and **B**. These two approaches are based on previous theoretical calculations reported by Houk et al., showing that there is a significant tendency for allylic bonds of acyclic alkenes to adopt a staggered arrangement with respect to the partially formed bonds in the transition states of related addition reactions.[23] Notably, they also established that there is a large conformational preference to place the bond between the largest group attached to the stereogenic carbon and this atom antiperiplanar to the forming bond.[23] It is also expected that the smallest group, i.e., the allylic hydrogen atom, occupies the inside position for the sake of minimizing steric interactions with the incoming dienophile as well as 1,3-allylic strain.[24] The same statements also have been furnished by the computed transition states of the cycloaddition reactions between polyenes and maleic anhydride.[25] As far as the approach of the dienophile is concerned, an *endo* attack is expected to be strongly preferred as a result of electrostatic repulsions between the lone pairs of the diazo group and the π-system of the diene in the alternative *exo* transition state (*exo-lone-pair effec*t).[26] The stereoselectivity deriving of this latter preference is not reflected in the structure of the reaction products when the dienophile is PTAD because the nitrogen centers of the triazolidine moiety undergo rapid inversion. Taking into account all previous considerations, we propose that the *endo* approach of the PTAD to conformer **A** for the less hindered side is the most favorable one (Scheme 6). In this model, the phenyl group at the allylic position is placed antiperiplanar to the approaching trajectory of the dienophile and the hydrogen atom is located in the inside position. Alternatively, the approach of the PTAD to the less hindered face of **B**, having the diene fragment rotated 180° with respect to **A**, would be less favored due to the presence in the corresponding transition state of more notable steric interactions between the incoming dienophile and the allylic methyl group, placed close to the forming cyclic framework. On the basis of this mechanistic scrutiny, the cycloadduct **8a** is expected to be the major diastereoisomer, as was experimentally observed (Scheme 6). To rationalize the diastereoselectivities observed for **4b** and **4c**, we have considered analogous approaches. The configurational assignment of **8b**/**8c** and **9b**/**9c** was performed on the basis of this assumption, and also by considering a similar steric requirement of the Me and CH_2OR groups.[27,28]

Computational Study

Computational Methods. All structures were optimized using the functional B3LYP[29] and the 6-31+G** basis set as implemented in the Gaussian03 suite of programs.[30] Density Functional Theory has been shown to reliably predict the results of [4+2] Diels−Alder and other pericyclic reactions.[31] All energy minima and transition structures were characterized by frequency analysis. The energies reported in this work include the zero-point vibrational energy corrections (ZPVE) and are not scaled. The intrinsic reaction coordinates (IRC)[32] were followed to verify the energy profiles connecting each transition

(21) (a) Tripathy, R.; Franck, R. W.; Onan, K. D. *J. Am. Chem. Soc.* **1988**, *110*, 3257−3262. (b) Fisher, M. J.; Hehre, W. J.; Kahn, S. D.; Overman, L. E. *J. Am. Chem. Soc.* **1988**, *110*, 4625−4633. (c) McDougal, P. G.; Jump, J. M.; Rojas, C.; Rico, J. G. *Tetrahedron Lett.* **1989**, *30*, 3897−3900. (d) Datta, S. C.; Franck, R. W.; Tripathy, R.; Quigley, G. J.; Huang, L.; Chen, S.; Sihaed, A. *J. Am. Chem. Soc.* **1990**, *112*, 8472−8478. (e) Adam, W.; Gläser, J.; Peters, K.; Prein, M. *J. Am. Chem. Soc.* **1995**, *117*, 9190−9193. (f) Crisp, G. T.; Gebauer, M. G. *J. Org. Chem.* **1996**, *61*, 8425−8431. (g) Ruijter, E.; Schültingkemper, H.; Wessjohann, L. A. *J. Org. Chem.* **2005**, *70*, 2820−2823.

(22) Kaila, N.; Franck, R. W.; Dannenberg, J. J. *J. Org. Chem.* **1989**, *54*, 4206−4212.

(23) (a) Caramella, P.; Rondan, N. G.; Paddon-Row, M. N.; Houk, K. N. *J. Am. Chem. Soc.* **1981**, *103*, 2438−2440. (b) Paddon-Row, M. N.; Rondan, N. G.; Houk, K. N. *J. Am. Chem. Soc.* **1982**, *104*, 7162−7166. (c) Houk, K. N.; Paddon-Row, M. N.; Rondan, N. G.; Wu, Y.-D.; Brown, F. K.; Spellmeyer, D. C.; Metz, J. T.; Li, Y.; Loncharich, R. J. *Science* **1986**, *231*, 1108−1117.

(24) (a) Johnson, F. *Chem. Rev.* **1968**, *68*, 375−413. (b) Hoffmann, R. W. *Chem. Rev.* **1989**, *89*, 1841−1860.

(25) Turner, C. I.; Paddon-Row, M. N.; Willis, A. C.; Sherburn, M. S. *J. Org. Chem.* **2005**, *70*, 1154−1163.

(26) (a) McCarrick, M. A.; Wu, Y.-D.; Houk, K. N. *J. Am. Chem. Soc.* **1992**, *114*, 1499−1500. (b) McCarrick, M. A.; Wu, Y.-D.; Houk, K. N. *J. Org. Chem.* **1993**, *58*, 3330−3343.

(27) Although steric effects depend so much upon the precise direction from which a reagent approaches that there can be no single scale for evaluating the effective size of a group, we assume that H < Me < Ph, see: Fleming, I.; Lewis, J. J. *J. Chem. Soc., Chem. Commun.* **1985**, 149−151.

(28) These steric requirements are based on *A* values, see: McGarvey, G. J.; Williams, J. M. *J. Am. Chem. Soc.* **1985**, *107*, 1435−1437.

(29) (a) Bartolotti, L. J.; Fluchichk, K. In *Reviews in Computational Chemistry*; Lipkowitz, K. B., Boyds, D. B., Eds.; VCH Publishers: New York, 1996; Vol. 7, pp 187−216. (b) Kohn, W.; Becke, A. D.; Parr, R. G. *J. Phys. Chem.* **1996**, *100*, 12974−12980. (c) Parr, R. G.; Pearson, R. G. *J. Am. Chem. Soc.* **1983**, *105*, 7512−7516. (d) Ziegler, T. *Chem. Rev.* **1991**, *91*, 651−667.

state to the correct local minima, by using the second-order Gonzalez−Schlegel integration method.[33] Wiberg bond orders[34] and natural atomic charges were calculated within the natural bond orbital (NBO) analysis.[35] The synchronicity of the reactions was determined by using a previously described approach.[36] The solvent effects have been considered by B3LYP/6-31+G** single-point calculations using a Self-Consistency Reaction Field (SCRF)[37] method, based on the Polarized Continuum Model (PCM)[38] of Tomasi and co-workers, in toluene and acetonitrile as solvents.

For simplicity, in order to model the reaction of PTAD with the thiazoles **1a**−**d** presented in the experimental part of this work, we selected as reactants the structurally simpler HTAD (**12**) and the four thiazoles **13a**−**d**. We have carried out an intensive exploration of the B3LYP/6-31+G** potential energy surfaces associated with the [4+2] cycloaddition reactions of HTAD with the thiazoles **13a**−**d** leading to the cycloadducts **14a**−**d**, respectively (Scheme 7).

Figure 1 displays the qualitative reaction profiles at the B3LYP/6-31+G** theoretical level and the location of the stationary points for the Diels−Alder reactions between HTAD and thiazoles **13a** and **13b**, while the qualitative reaction profiles corresponding to the reactions of HTAD with the thiazoles **13b**−**d**, though the intermediates **INT1b**,**c** and **INT2d**, are shown in

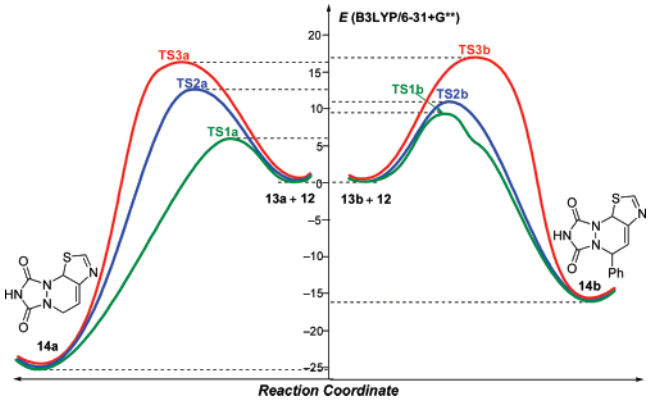

FIGURE 1. Qualitative reaction profiles at the B3LYP/6-31+G** level of the reactions between HTAD (**12**) and the thiazoles **13a** and **13b** leading to the cycloadducts **14a** and **14b**, respectively, through the transition states **TS1a**,**b**, **TS2a**,**b,** and **TS3a**,**b**.

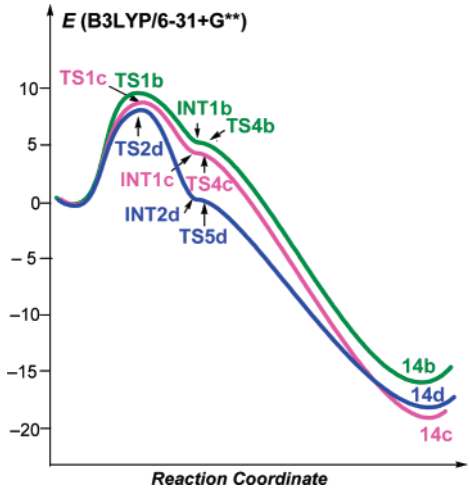

FIGURE 2. Qualitative reaction profiles at the B3LYP/6-31+G** level of the reactions between HTAD (**12**) and the thiazoles **13b**−**d** leading to the cycloadducts **14b**−**d** through the dipolar intermediates **INT1b**,**c** and **INT2d**, respectively.

Figure 2. Figures 3 and 4 show the geometries of the relevant stationary points (excluding reactants and cycloadducts), including the most significant bond distances. Table 4 contains the relative and free energies of the stationary points at the B3LYP/6-31+G** theoretical level and selected geometrical and electronic parameters. In Table 5 the static global properties (electronic chemical potential μ, chemical hardness η, and global electrophilicity ω) of HTAD and the thiazoles **13a**−**d** are displayed. We will comment only on the electronic energies, unless otherwise stated.

For the Diels−Alder reaction of HTAD with **13a** and **13b**, two *endo* (**TS1a**,**b** and **TS2a**,**b**) and one *exo* (**TS3a**,**b**) transition structures were located. The difference between the two *endo* transition structures **TS1** and **TS2** relies simply in which of the forming C−N bonds is more advanced. Thus, whereas in **TS1** the more advanced forming bond is C5−N, in **TS2** it is instead the C1−N bond (see Table 4).

The *exo* transition structures were higher in energy than their *endo* counterparts. As stated above, the preference for *endo* transition structures can be easily explained on the basis of the *exo-lone-pair effect* in hetero-Diels−Alder reactions.[26] Accordingly, in the *exo* transition structures **TS3a**,**b**, the lone pairs at

(30) Frisch, M. J.; Trucks, G. W.; Schlegel, H. B.; Scuseria, G. E.; Robb, M. A.; Cheeseman, J. R.; Montgomery, J. A., Jr.; Vreven, T.; Kudin, K. N.; Burant, J. C.; Millam, J. M.; Iyengar, S. S.; Tomasi, J.; Barone, V.; Mennucci, B.; Cossi, M.; Scalmani, G.; Rega, N.; Petersson, G. A.; Nakatsuji, H.; Hada, M.; Ehara, M.; Toyota, K.; Fukuda, R.; Hasegawa, J.; Ishida, M.; Nakajima, T.; Honda, Y.; Kitao, O.; Nakai, H.; Klene, M.; Li, X.; Knox, J. E.; Hratchian, H. P.; Cross, J. B.; Adamo, C.; Jaramillo, J.; Gomperts, R.; Stratmann, R. E.; Yazyev, O.; Austin, A. J.; Cammi, R.; Pomelli, C.; Ochterski, J. W.; Ayala, P. Y.; Morokuma, K.; Voth, G. A.; Salvador, P.; Dannenberg, J. J.; Zakrzewski, V. G.; Dapprich, S.; Daniels, A. D.; Strain, M. C.; Farkas, O.; Malick, D. K.; Rabuck, A. D.; Raghavachari, K.; Foresman, J. B.; Ortiz, J. V.; Cui, Q.; Baboul, A. G.; Clifford, S.; Cioslowski, J.; Stefanov, B. B.; Liu, G.; Liashenko, A.; Piskorz, P.; Komaromi, I.; Martin, R. L.; Fox, D. J.; Keith, T.; Al-Laham, M. A.; Peng, C. Y.; Nanayakkara, A.; Challacombe, M.; Gill, P. M. W.; Johnson, B.; Chen, W.; Wong, M. W.; Gonzalez, C.; Pople, J. A. *Gaussian 03*, Revision B.03; Gaussian, Inc.: Pittsburgh, PA, 2003.

(31) See for example: (a) Goldstein, E.; Beno, B.; Houk, K. N. *J. Am. Chem. Soc.* **1996**, *118*, 6036−6043. (b) Wiest, O.; Montiel, D. C.; Houk, K. N. *J. Phys. Chem. A* **1997**, *101*, 8378−8388. (c) Garcia, J. I.; Martinez-Merino, V.; Mayoral, J. A.; Salvatella, L. *J. Am. Chem. Soc.* **1998**, *120*, 2415−2420. (d) Domingo, L. R.; Arnó, M.; Andrés, J. *J. Am. Chem. Soc.* **1998**, *120*, 1617−1618. (e) Liu, J.; Niwayama, S.; You, Y.; Houk, K. N. *J. Org. Chem.* **1998**, *63*, 1064−1073. (f) Birney, D. M. *J. Am. Chem. Soc.* **2000**, *122*, 10917−10925.

(32) (a) Fukui, K. *J. Phys. Chem.* **1970**, *74*, 4161−4162. (b) Fukui, K. *Acc. Chem. Res.* **1981**, *14*, 363−368.

(33) (a) Gonzalez, C.; Schlegel, H. B. *J. Phys. Chem.* **1990**, *94*, 5523−5527. (b) Gonzalez, C.; Schlegel, H. B. *J. Chem. Phys.* **1991**, *95*, 5853−5860.

(34) Wiberg, K. B. *Tetrahedron* **1968**, *24*, 1083−1096.

(35) (a) Reed, A. E.; Weinstock, R. B.; Weinhold, F. *J. Chem. Phys.* **1985**, *83*, 735−746. (b) Reed, A. E.; Curtiss, L. A.; Weinhold, F. *Chem. Rev.* **1988**, *88*, 899−926. (c) Reed, A. E.; Schleyer, P. v. R. *J. Am. Chem. Soc.* **1990**, *112*, 1434−1445.

(36) (a) Borden, W. T.; Loncharich, R. J.; Houk, K. N. *Annu. Rev. Phys. Chem.* **1988**, *39*, 213−236. (b) Moyano, A.; Pericas, M. A.; Valenti, E. *J. Org. Chem.* **1989**, *54*, 573−582. (c) These indexes also have been used to characterize cycloaddition reactions other than [4+2], see for example: Lecea, B.; Ayerbe, M.; Arrieta, A.; Cossío, F. P.; Branchadell, V.; Ortuño, R. M.; Baceiredo, A. *J. Org. Chem.* **2007**, *72*, 357−366.

(37) (a) Tomasi, J.; Persico, M. *Chem. Rev.* **1994**, *94*, 2027−2094. (b) Simkin, B. Y.; Sheikhet, I. *Quantum Chemical and Statical Theory of Solutions−A Computational Approach*; Ellis Horwood: London, UK, 1995; pp 78−101.

(38) (a) Miertus, S.; Scrocco, E.; Tomasi, J. *Chem. Phys.* **1981**, *55*, 117−129. (b) Cammi, R.; Tomasi, J. *J. Chem. Phys.* **1994**, *100*, 7495−7502. (c) Barone, V.; Cossi, M.; Tomasi, J. *J. Chem. Phys.* **1997**, *107*, 3210−3221.

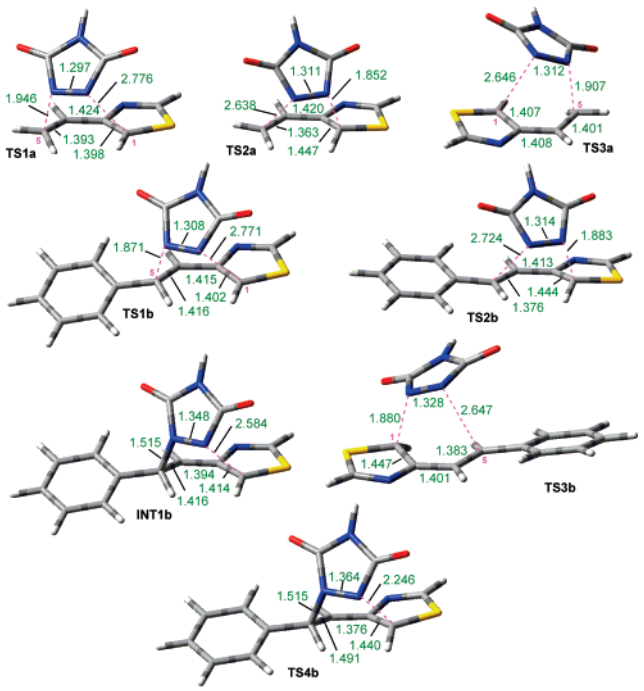

FIGURE 3. B3LYP/6-31+G**-optimized geometries showing relevant bond distances of the stationary points found in the reactions of HTAD (**12**) with the thiazoles **13a**,**b** leading to the [4+2] cycloadducts **14a**,**b**.

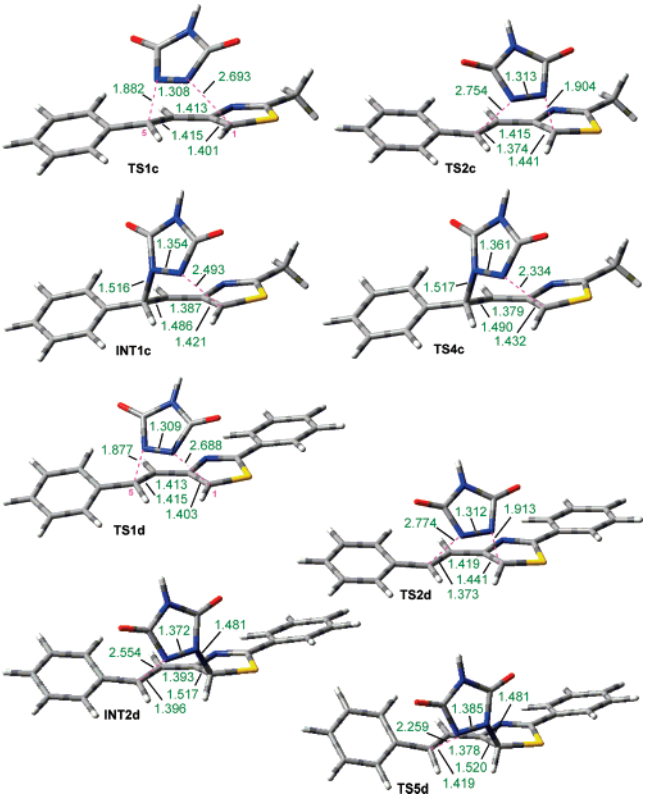

FIGURE 4. B3LYP/6-31+G**-optimized geometries showing relevant bond distances of the stationary points found in the reactions of HTAD (**12**) with the thiazoles **13c**,**d** leading to the [4+2] cycloadducts **14c**,**d**.

the two double bonded nitrogen atoms of HTAD, which are *endo* positioned with respect to the diene π-system, induce a massive destabilizing effect. Similar results have been reported

TABLE 4. Relative Energies with Zero-Point Vibrational Energy Corrections (kcal·mol^{-1}), Relative Free Energies (kcal·mol^{-1}), Bond Distances (*d*, in Å), and Bond Orders (BO) of the Forming C−N Bonds, and Synchronicities (Sy), Calculated at the B3LYP/6-31+G// B3LYP/6-31+G** Theoretical Level for the Stationary Points Found in the Diels−Alder Reactions of HTAD with the Thiazoles 13a−d Leading to the Cycloadducts 14a−d**

structure	rel energy	rel free energy	C1−N *d*/BO	C5−N *d*/BO	Sy
TS1a (*endo*)	6.37	20.00	2.776/0.09	1.946/0.43	0.72
TS2a (*endo*)	13.04	27.29	1.852/0.52	2.638/0.14	0.73
TS3a (*exo*)	16.29	29.77	2.646/0.14	1.907/0.49	0.80
14a	−25.46	−10.78	1.456/0.94	1.460/0.94	
TS1b (*endo*)	9.58	23.97	2.771/0.11	1.871/0.49	0.73
INT1b	5.75	19.73	2.584/0.17	1.515/0.85	
TS4b	6.05	21.33	2.246/0.32	1.515/0.86	
TS2b (*endo*)	10.31	24.65	1.883/0.50	2.724/0.11	0.74
TS3b (*exo*)	17.32	31.14	1.880/0.14	2.647/0.52	0.74
14b	−16.45	−1.68	1.420/0.99	1.487/0.92	
TS1c (*endo*)	8.63	23.50	2.693/0.12	1.882/0.48	0.73
INT1c	4.45	18.87	2.493/0.21	1.516/0.86	
TS4c	4.52	20.89	2.334/0.27	1.517/0.86	
TS2c (*endo*)	8.23	22.92	1.904/0.48	2.754/0.11	0.72
14c	−18.45	−3.05	1.423/0.99	1.487/0.92	
TS1d (*endo*)	8.80	23.60	2.688/0.12	1.877/0.49	0.75
TS2d (*endo*)	8.20	22.79	1.913/0.47	2.774/0.10	0.72
INT2d	0.60	15.23	1.481/0.91	2.554/0.19	
TS5d	0.83	16.75	1.481/0.91	2.259/0.32	
14d	−17.97	−2.75	1.423/0.99	1.487/0.92	

TABLE 5. Calculated Values of Electrophilicity (ω, in eV), Electronic Chemical Potential (μ, in au), and Chemical Hardness (η, in au) for HTAD (12) and Thiazoles 13a−d

	ω	μ	η	$\Delta\omega$ ($\omega_{12}-\omega_{13}$)
12	5.4355	−0.2262	0.1281	
13a	1.6400	−0.1469	0.1789	3.80
13b	1.8571	−0.1421	0.1480	3.58
13c	1.7864	−0.1380	0.1450	3.65
13d	1.9574	−0.1408	0.1378	3.48

by Houk in the computational study of the Diels−Alder reaction of HTAD with butadiene.[13a,c]

For the reaction of HTAD with 4-vinylthiazole (**13a**), **TS1a** is the lowest in energy (6.4 kcal/mol up to reactants), whereas the other *endo* transition state (**TS2a**) is 13.0 kcal·mol^{-1} higher in energy than the reactants. However, after including the entropy correction, the free energies turned out to be 20.0 and 27.3 kcal·mol^{-1} for **TS1a** and **TS2a**, respectively (see Table 4). The difference in energy between these *endo* transition structures and *exo* **TS3a** is 9.92 kcal·mol^{-1} between **TS1a** and **TS3a** and 3.25 kcal·mol^{-1} between **TS2a** and **TS3a**. From these calculations it seems clear that the preferred channel for the formation of cycloadduct **13a** is via **TS1a**. For the reaction of HTAD with **13b** the energy difference between both *endo* transition states, **TS1b** and **TS2b**, is only 0.7 kcal·mol^{-1}, lower than in the preceding reaction, again **TS2b** being higher in energy than **TS1b**. The preference for *endo* transition structures still dominates with an energy difference of 7.74 kcal·mol^{-1} between **TS1b** and **TS3b** and 7.01 kcal·mol^{-1} between **TS2b** and **TS3b**.[39]

Interestingly, there is a significant twisting between the diene fragment of the thiazole and the HTAD ring in the four *endo* transition structures, the HTAD ring being tilted 47−50° relative to the plane of the diene fragment. In contrast, the *exo* transition

(39) Whereas in *exo*-**TS3a** the more advanced forming bond is C5−N, in *exo*-**TS3b** it is the C1−N bond. We have located another *exo* transition state for the reaction of HTAD with **13b** where the more advanced forming bond is C5−N, but it is higher in energy than *exo*-**TS3b**, see the Supporting Information. In contrast, for the reaction of HTAD with **13a** we have only found one *exo* transition state, *exo*-**TS3a**.

structures **TS3a**,**b** show less significant twisting (see Table S1 in the Supporting Information).[40]

With these results in hand, and taking into account the *exo-lone-pair effect* (see above), we have not optimized the corresponding *exo* transition states for the reactions of HTAD with the thiazoles **13c** and **13d**, studying in depth only the *endo* approaches. The substitution of the hydrogen atom at the 2-position of the thiazole ring in **13b** by a methyl or a phenyl group (thiazoles **13c** and **13d**) leads to slight decreases in the energies of the respective two *endo* transition structures (**TS1c**,**d** and **TS2c**,**d**). The transition states **TS2c**,**d** are lower in energy than **TS1c**,**d**, in sharp contrast with the previous results found in the reactions of **13a**,**b**, where **TS1a**,**b** are less energetic than **TS2a**,**b**. Due to the small energy differences between **TS1b**−**d** and **TS2b**−**d** the formation of **14b**−**d** may well take place by any of these two competitive channels.

All these reactions are exothermic processes, their reaction energies being in the range of −16.4 to −25.46 kcal·mol^{-1}. In all the computed reactions, the two types of located *endo* transition structures, **TS1a**−**d** and **TS2a**−**d**, are highly asynchronous. This is not surprising because even the reaction of HTAD with butadiene, in spite of the symmetry of both reactants, has been described to proceed through a highly unsymmetrical and asynchronous transitions state.[13] As introduced above, whereas in **TS1a**−**d** the formation of the bond between the exocyclic terminal carbon atom of the diene fragment and the nitrogen atom (C5−N bond) is notably more advanced compared to that between the second nitrogen atom and the endocyclic terminal carbon atom (C1−N bond), the opposite is found in **TS2a**−**d**. Thus, the C1−N and C5−N bond distances in **TS1a**−**d** range from 2.69 to 2.78 Å and 1.87 to 1.95 Å, respectively. In contrast, the same bond distances in **TS2a**−**d** are between 1.85 and 1.91 Å (C1−N) and between 2.64 and 2.75 Å (C5−N).

Compared with the bond distance, the bond order (BO)[34] is a more balanced measure of the extent of a bond-formation or bond-breaking process along a reaction pathway. This theoretical tool, quite common in the computational study of reaction mechanisms,[41] also has been successfully used for characterizing polar Diels−Alder reactions.[42] We have computed the Wiberg bond indexes by using the NBO method. The BO values of the C1−N and C5−N forming bonds for each transition state, listed in Table 4, show that whereas in **TS1a**−**d** the C5−N bond is partially formed (the BO ranging from 0.43 to 0.49) there is little bonding between C1 and the second nitrogen atom (the BO varying from 0.09 to 0.12). Inversely, in **TS2a**−**d** the C5−N and C1−N BOs range from 0.10 to 0.14 and from 0.47 to 0.52, respectively. To obtain a precise measure of the relative asynchronicities of these Diels−Alder reactions, we have also calculated their synchronicity values (Sy) included in Table 4. Whereas for a perfectly synchronous reaction Sy = 1, the values obtained for the reactions of HTAD with **13a**−**d** through the different transition states are quite similar and close to 0.7.

Natural population analysis[35a,b] allows the evaluation of the charge transfer along the cycloaddition reactions. It has been suggested that the feasibility of a Diels−Alder reaction is related to the charge transfer along the bond-forming processes, in correspondence with the more or less polar character of these reactions.[42a,c,43] The B3LYP/6-31+G** natural atomic charges at the transition states show the charge transferred from the donor thiazole to the acceptor HTAD. The values of the charge transferred from **13a**−**d** to **12** vary from 0.34e to 0.47e (see Table S1 in the Supporting Information). These data reveal that HTAD is acting as an electron acceptor and the thiazoles **13a**−**d** as electron donors as the charge transfer fluxes from the dienes to the dienophile.

Both theoretical tools, charge transfers and bond orders, indicate that these cycloaddition reactions, taking place via highly asynchronous transition states, are polar processes characterized by the nucleophilic attack of the thiazole to the N═N double bond of HTAD. The same conclusions can be reached from the analysis of the values of the static global properties (electronic chemical potential μ, chemical hardness η, and global electrophilicity, ω) of both reaction partners. These electronic indexes, as defined within the DFT of Pearson, Parr, and Yang,[29c,44] are useful tools for understanding the reactivity of molecules in their ground states. Thus, the electronic chemical potential μ describes the changes in electronic energy with respect to the number of electrons, and it is usually associated with the charge transfer ability of the system in its ground state geometry. Apart from this value, it is also possible to obtain a quantitative estimation of the chemical hardness concept introduced by Pearson[29c,44,45] by calculating the η index. Finally, Parr et al.[46] have introduced a useful definition of global electrophilicity (ω), which measures the stabilization in energy when the system acquires an additional electronic charge ΔN from the environment. In fact, this index has been extensively used by Domingo[42c,43,47] and others[42b] to classify dienes and dienophiles on a unique scale of electrophilicity.[48] Additionally, the more or less polar character of a cycloaddition reaction[36c] can be measured as the difference between the electrophilicities of diene and dienophile. All these indexes (μ, η, and ω) can be calculated by solving very simple operational equations, as defined in eqs 1−3, in terms of the one-electron energies of the HOMO (E_H) and LUMO (E_L) frontier molecular orbitals.[29d,44]

$$\omega = \frac{\mu^2}{2\eta} \tag{1}$$

$$\mu \approx \frac{(E_H + E_L)}{2} \tag{2}$$

$$\eta \approx E_L - E_H \tag{3}$$

(40) A similar difference in the degree of twisting has been reported by Houk for the *endo* and *exo* transition states computed for the Diels−Alder reaction of HTAD with butadiene, see ref 13a.

(41) (a) Varandas, A. J. C.; Formosinho, S. J. F. *J. Chem. Soc., Faraday Trans. 2* **1986**, *82*, 953−962. (b) Lendvay, G. *THEOCHEM* **1988**, *167*, 331−338. (c) Lendvay, G. *J. Phys. Chem.* **1989**, *93*, 4422−4429. (d) Lendvay, G. *J. Phys. Chem.* **1994**, *98*, 6098−6104.

(42) See for example: (a) Domingo, L. R.; Arnó, M.; Andrés, J. *J. Org. Chem.* **1999**, *64*, 5867−5875. (b) Gómez-Bengoa, E.; Helm, M.; Plant, A.; Harrity, J. P. A. *J. Am. Chem. Soc.* **2007**, *129*, 2691−2699. (c) Domingo, L. R. *Tetrahedron* **2002**, *58*, 3765−3774.

(43) Domingo, L. R.; Aurell, M. J.; Pérez, P.; Contreras, R. *J. Org. Chem.* **2003**, *68*, 3884−3890.

(44) Parr, R. G.; Yang, W. *Density Functional Theory of Atoms and Molecules*; Oxford University: New York, 1989.

(45) Pearson, R. G. *Chemical Hardness, Applications from Molecules to Solids*; Wiley-VCH Verlag GMBH: Weinheim, Germany, 1997.

(46) Parr, R. G.; von Szentpaly, L.; Liu, S. *J. Am. Chem. Soc.* **1999**, *121*, 1922−1924.

(47) (a) Domingo, L. R.; Arnó, M.; Contreras, R.; Pérez, P. *J. Phys. Chem. A* **2002**, *106*, 952−961. (b) Domingo, L. R.; Aurell, M. J. *J. Org. Chem.* **2002**, *67*, 959−965. (c) Domingo, L. R.; Asensio, A.; Arroyo, P. *J. Phys. Org. Chem.* **2002**, *15*, 660−666. (d) Domingo, L. R.; Aurell, M. J; Pérez, P.; Contreras, R. *J. Phys. Chem. A* **2002**, *106*, 6871−6875.

(48) Domingo, L. R.; Aurell, M. J.; Pérez, P.; Contreras, R. *Tetrahedron* **2002**, *58*, 4417−4423.

The electronic chemical potential of HTAD[49] (**12**) (μ = −0.2262 au) is lower than those of the thiazoles **13a**−**d** (see Table 5), thereby indicating that the net charge transfer should take place from the thiazole toward HTAD, as expected for a Diels−Alder reaction of normal-electron demand. These results are in agreement with the charge-transfer analysis shown above. It is worth noting the very high value of the electrophilicity index for HTAD (ω = 5.44 eV).[50] On the other hand, the large values of the electrophilicity differences, $\Delta\omega$, indicate the highly polar character of these cycloaddition reactions, which can be compared with the low value computed for the prototypical Diels−Alder cycloaddition between butadiene and ethylene ($\Delta\omega$ = 0.32 eV).[50]

The high degree of asynchronicity of the processes described herein led us to explore more intensively their potential energy surfaces in search of stepwise mechanisms. Moreover, intrinsic reaction coordinates (IRC) calculations were used to follow all reaction pathways, showing the connection of each transition state with the reactants. The IRC paths in the forward direction stop in geometries where the more advanced $C_{diene}-N_{dienophile}$ bond in the transition state reaches a distance close to 1.5 Å and the distance of the other forming C−N bond is longer than 2.4 Å. In general, optimization of these structures led to the final cycloadducts **14a**−**d** except for the IRC calculations of **TS1b**, **TS1c**, and **TS2d**, where such optimization led to the three dipolar intermediates **INT1b**, **INT1c**, and **INT2d**, respectively. The transition states **TS4b**, **TS4c**, and **TS5d** connecting these intermediates with the cycloadducts **14b**, **14c**, and **14d** could also be located, showing only one imaginary frequency corresponding to either the C1−N (**TS4b**,**c**) or C5−N (**TS5d**) bond formation. **INT1b** and **INT1c** are respectively 3.83 and 4.17 kcal·mol^{-1} lower in energy than **TS1b** and **TS1c**, whereas the energy of **INT2d** is lower than that of **TS2d** by 7.60 kcal·mol^{-1}. In short, the reaction channels leading to cycloadducts **14b**−**d** via the transition states **TS1b**, **TS1c**, and **TS2d** are thus characterized as stepwise mechanisms involving the dipolar intermediates **INT1b**, **INT1c**, and **INT2d**. CASSCF[51](6,6)/6-31G*//B3LYP/6-31+G** calculations were performed in order to check if these intermediates show biradical characteristics. The results show that the closed-shell S_0 wave function is largely the predominant one (92−94%). Therefore, these intermediates are adequately described by a single reference wave function.

The energy barriers for their cyclization through **TS4b**,**c** and **TS5d** are only 0.3, 0.07, and 0.23 kcal·mol^{-1}, respectively, virtually nonexistent. Consequently, the potential energy surfaces around the polar intermediates **INT1b**,**c** and **INT2d** and the transition states **TS4b**,**c** and **TS5d** can be qualified as very flat (see Figure 2), suggesting that intermediates **INT1b**, **INT1c**, and **INT2d** must have a very short half-life. In fact, their geometries, highly preorganized to undergo easily the cyclization, endorse this assumption.

To evaluate the solvent influence in these cycloadditions we have carried out single-point calculations by using the Polarized Continuum Model (PCM), including two solvents of increasing polarity (toluene and acetonitrile), for the two *endo* approaches found in the Diels−Alder reactions of HTAD with 4-styryl-1,3-thiazole (**13b**) at the B3LYP/6-31+G** level. With the inclusion of these solvents, transition states and intermediates are similarly stabilized relative to reactants, and thus the barriers are not significantly affected. The product is slightly destabilized in relation to the reactants, and consequently the exothermicity of the reaction is now somewhat lower than that in the gas phase (see Table S6 in the Supporting Information). These results likely can be extended to the rest of the cycloadditions considered in this computational study.

We could not locate analogous polar intermediates or transition states in the rest of the reaction channels indicating that those other Diels−Alder reactions occur by concerted mechanisms through very polar and asynchronous transition states, and that the formation of the less advanced C−N bond takes place downhill from the transition states toward the cycloadducts.

Summarizing, this computational study shows that the scrutinized hetero-Diels−Alder reactions can be considered very asynchronous and polar processes. A complete analysis of the computed transition states indicates that these processes are characterized by the charge transfer from the diene (the thiazoles **13a**−**d**) to the electron-poor triazoline. There are two *endo* approaches differing on which forming C−N bond is more advanced. They are energetically preferred over the *exo* transition states due to the *exo-lone-pair effect*. In spite of the markedly polar character and the high asynchronicity of these processes, they take place in a concerted fashion, except in a few cases occurring in a stepwise manner with the intervention of dipolar intermediates which transit very easily to the final cycloadducts.

Conclusions

4-Alkenylthiazoles behave as inner−outer dienes in their reactions with PTAD to give the corresponding cycloadducts in good yields and excellent levels of stereocontrol. The stereochemistry of the reaction products indicates that the approach of the dienophile to the dienes takes place suprafacially. The presence of a stereogenic center attached to the terminal carbon atom of the diene moderately controls the facial diastereoselectivity. The stereochemical course of these processes is dominated by the steric interactions featured by both diastereomeric transition states. Finally, the computational study by using structurally simpler reagents indicates that, in most cases, these reactions take place in a concerted fashion. They show polar character and are highly asynchronous, taking place through *endo* transition states. In a few cases, the intervention of dipolar intermediates was observed, although they cyclize to the final adducts practically without energetic cost.

Experimental Section

General Procedure for the Synthesis of the Cycloadducts 2. PTAD (0.13 g, 0.75 mmol) was added to a solution of the corresponding 4-alkenylthiazole **1**[16] (0.75 mmol) in toluene (5 mL). After 5 min of stirring at room temperature, a white solid precipitated from the solution, which was isolated by filtration. Another crop was collected from the mother liquors by adding Et_2O (2 mL) to the residue, obtained after removal of the solvent, and subsequent filtration of the resulting solid.

(5*R,10a*R**)-5-(4-Chlorophenyl)-2,8-diphenyl-5,10a-dihydrothiazolo[5,4-*c*][1,2,4]triazolo[1,2-*a*]pyridazin-7,9-dione (2a).** Yield

(49) A detailed study on the geometric and electronic features of HTAD can be found in: Anas, S.; Krishnan, K. S.; Sajisha, V. S.; Anju, K. S.; Radhakrishnan, K. V.; Suresh, E.; Suresh, C. H. *New J. Chem.* **2007**, *31*, 237−246.

(50) Compare with the values of the global electrophilicity indexes of strong electrophiles in ref 48.

(51) (a) Hegarty, D.; Robb, M. A. *Mol. Phys.* **1979**, *38*, 1795−1812. (b) Eade, R. H. E.; Robb, M. A. *Chem. Phys. Lett.* **1981**, *83*, 362−368. (c) Schlegel, H. B.; Robb, M. A. *Chem. Phys. Lett.* **1982**, *93*, 43−46.

>99%; mp 174−176 °C (colorless prisms, $CHCl_3/Et_2O$); IR (nujol) 1785, 1714, 1545, 1506, 1492, 1426, 1269, 1145, 1269, 1145, 769, 692 cm^{-1}; ^1H NMR ($CDCl_3$) δ 5.83 (t, 1H, J = 3.5 Hz), 6.02 (t, 1H, J = 3.0 Hz), 6.11 (dd, 1H, J = 3.8 Hz, J = 2.9 Hz), 7.32−7.36 (m, 3H), 7.40−7.45 (m, 6H), 7.47−7.51 (m, 2H), 7.55−7.60 (m, 1H), 7.94−7.97 (m, 2H); ^{13}C NMR ($CDCl_3$) δ 56.1 (d), 65.4 (d), 116.2 (d), 125.0 (2 × d), 128.40 (d), 128.41 (2 × d), 128.9 (2 × d), 129.08 (2 × d), 129.12 (2 × d), 129.8 (2 × d), 130.6 (s), 132.0 (s), 132.9 (d), 134.5 (s), 135.2 (s), 149.8 (s), 153.6 (s), 155.1 (s), 173.9 (s). MS (EI, 70 eV) *m*/*z* (rel intensity) 472 (M^+, 1), 299 (25), 298 (25), 297 (68), 296 (40), 194 (46), 177 (30), 149 (45), 121 (100), 119 (88), 115 (72), 104 (33), 91 (52), 64 (39). Anal. Calcd for $C_{25}H_{17}ClN_4O_2S$ (472.95): C, 63.49; H, 3.62; N, 11.85; S, 6.78. Found: C, 63.23; H, 3.72; N, 11.89; S, 6.90.

(4*R,5*R**)-5-(4-Chlorophenyl)-2,8-diphenyl-4-(4-phenyl-3,5-dioxo-1,2,4-triazolidin-1-yl)-4,5-dihydrothiazolo[5,4-*c*][1,2,4]-triazolo[1,2-*a*]pyridazin-7,9-dione (3a).** PTAD (0.02 g, 0.11 mmol) was added to a solution of **2a** (0.05 g, 0.11 mmol) in toluene (5 mL). The reaction mixture was stirred under reflux for 20 min. After removal of the solvent under reduced pressure, the residue was purified by silica gel column chromatography eluting with 1:1 AcOEt/hexane (R_f 0.33). Yield 97%; mp 164−166 °C (colorless prisms, $CHCl_3/Et_2O$); IR (nujol) 1781, 1725, 1563, 1500, 1410, 760, 690 cm^{-1}; ^1H NMR ($CDCl_3$) δ 5.89 (broad s, 1H), 5.95 (d, 1H, J = 1.4 Hz), 7.20 (d, 2H, J = 8.6 Hz), 7.31 (d, 2H, J = 8.6 Hz), 7.33−7.44 (m, 13H), 7.84−7.86 (m, 2H), 8.67 (broad s, 1H, NH); ^{13}C NMR ($CDCl_3$) δ 55.2 (d), 59.4 (d), 125.4 (2 × d), 125.6 (2 × d), 126.4 (2 × d), 128.2 (2 × d), 128.5 (d), 128.8 (d), 129.2 (2 × d), 129.25 (2 × d), 129.32 (2 × d), 129.6 (s), 129.7 (2 × d), 130.0 (s), 130.3 (s), 130.5 (s), 130.9 (d), 132.3 (s), 132.5 (s), 135.8 (s), 146.0 (s), 149.6 (s), 152.9 (s), 153.7 (s), 162.5 (s). MS (EI, 70 eV) *m*/*z* (rel intensity) 648 (M^+ + 1, 15), 473 (43), 471 (90), 393 (49), 322 (92), 149 (100), 109 (53), 107 (47). Anal. Calcd for $C_{33}H_{22}ClN_7O_4S$ (648.09): C, 61.16; H, 3.42; N, 15.13; S, 4.95. Found: C, 60.83; H, 3.59; N, 15.29; S, 5.07.

General Procedure for the Preparation of α-Chloroketones 7a−c. The corresponding aldehyde **6** (14.15 mmol) was added to a suspension of **5**[52] (2.00 g, 2.83 mmol) in dry toluene (25 mL) and the reaction mixture was stirred at room temperature or 40 °C (for exact temperature and reaction times see every particular case in Table 2). After removal of all volatiles under reduced pressure, the residue was purified by silica gel column chromatography.

(*E*)-1-Chloro-5-phenyl-3-hexen-2-one (7a). Temperature and reaction time: 25 °C, 7 days. AcOEt/hexane (1:5) was used as eluent (R_f 0.63). Yield 80% (yellow liquid); IR (neat) 1712, 1697, 1626, 1601, 1493, 1452, 1399, 1292, 1177, 1076, 1013, 978, 761, 700 cm^{-1}; ^1H NMR ($CDCl_3$) δ 1.44 (d, 3H, J = 6.9 Hz), 3.65 (quintd, 1H, J = 6.9 Hz, J = 1.5 Hz), 4.20 (s, 2H), 6.27 (dd, 1H, J = 15.9 Hz, J = 1.5 Hz), 7.11 (dd, 1H, J = 15.9 Hz, J = 6.9 Hz), 7.16−7.23 (m, 2H), 7.24−7.27 (m, 1H), 7.29−7.35 (m, 2H); ^{13}C NMR ($CDCl_3$) δ 20.0 (q), 42.3 (d), 47.0 (t), 124.5 (d), 126.9 (d), 127.2 (2 × d), 128.7 (2 × d), 142.6 (s), 153.5 (d), 191.2 (s). MS (EI, 70 eV) *m*/*z* (rel intensity) 210 (M^+ + 2, 17), 208 (M^+, 54), 173 (46), 159 (89), 144 (64), 141 (53), 134 (45), 131 (100), 129 (95), 116 (46), 115 (55), 105 (74), 103 (44), 91 (58), 79 (41), 77 (62). HRMS (EI): *m*/*z* calcd for $C_{12}H_{13}ClO$ 208.065493, found 208.065532.

General Procedure for the Preparation of 4-Alkenylthiazoles 4a−c. Thiobenzamide (0.62 g; 4.50 mmol) was added to a solution of the corresponding α-haloketone **7** (3.00 mmol) in ethanol (50 mL) and the reaction mixture was stirred under reflux for 5 h. The solvent was removed under reduced pressure and 5% $NaHCO_3$ aqueous solution (50 mL) was added. Then, the reaction mixture was extracted with CH_2Cl_2 (3 × 50 mL). The combined organic extracts were dried with $MgSO_4$. The solvent was removed and the residue was purified by silica gel column chromatography.

2-Phenyl-4-[(*E*)-3-phenyl-1-butenyl]thiazole (4a).[53] AcOEt/hexane (1:20) was used as eluent (R_f 0.36). Yield 63%; yellow oil; IR (neat) 1488, 1451, 1275, 1107, 1003, 967, 762, 690 cm^{-1}; ^1H NMR ($CDCl_3$) δ 1.41 (d, 3H, J = 7.0 Hz), 3.59 (quintd, 1H, J = 6.9 Hz, J = 1.3 Hz), 6.35 (dd, 1H, J = 15.6 Hz, J = 1.3 Hz), 6.80 (dd, 1H, J = 15.6 Hz, J = 6.8 Hz), 6.88 (s, 1H), 7.11−7.15 (m, 1H), 7.20−7.26 (m, 4H), 7.30−7.34 (m, 3H), 7.86−7.88 (m, 2H); ^{13}C NMR ($CDCl_3$) δ 21.1 (q), 42.4 (d), 113.6 (d), 121.8 (d), 126.2 (d), 126.6 (2 × d), 127.4 (2 × d), 128.5 (2 × d), 128.8 (2 × d), 129.9 (d), 133.6 (s), 138.5 (d), 145.3 (s), 155.0 (s), 167.7 (s). MS (EI, 70 eV) *m*/*z* (rel intensity) 291 (M^+, 46), 238 (32), 217 (30), 188 (30), 135 (100), 105 (69), 103 (53), 77 (61).

General Procedure for the Synthesis of the PTAD Adducts 8 and 9. PTAD (0.13 g, 0.75 mmol) was added to a solution of the corresponding 4-alkenylthiazole **4** (0.75 mmol) in toluene (5 mL), precooled at −5 °C. The reaction mixture was stirred at the same temperature for 30 min. The solvent was removed under reduced pressure and the residue purified by silica gel column chromatography. Only the mixture of diastereoisomers **8a** and **9a** could be resolved. The other two examples, **8b**/**9b** and **8c**/**9c**, were isolated as diastereomeric mixtures (Supporting Information).

(5*R,10a*S**)-2,8-Diphenyl-5-[(1*S**)-1-phenylethyl]-5,10a-dihydrothiazolo[5,4-*c*][1,2,4]triazolo[1,2-*a*]pyridazin-7,9-dione (8a).** AcOEt/hexane (1:2) was used as eluent (R_f 0.30). Yield 62%; mp 151−153 °C (colorless prisms, $CHCl_3/Et_2O$); IR (nujol) 1771, 1709, 1541, 1419, 1273, 953, 852, 759, 684 cm^{-1}; ^1H NMR ($CDCl_3$) δ 1.45 (d, 3H, J = 7.3 Hz), 3.81 (quint, 1H, J = 7.0 Hz), 5.09 (dt, 1H, J = 6.2 Hz, J = 3.5 Hz), 5.70 (t, 1H, J = 3.0 Hz), 6.30 (dd, 1H, J = 3.6 Hz, J = 2.9 Hz), 7.10−7.12 (m, 2H), 7.20−7.24 (m, 3H), 7.39−7.57 (m, 8H), 7.87−7.89 (m, 2H); ^{13}C NMR ($CDCl_3$) δ 17.4 (q), 41.8 (d), 57.6 (d), 64.5 (d), 113.8 (d), 125.3 (2 × d), 127.6 (d), 128.2 (4 × d), 128.4 (3 × d), 128.8 (2 × d), 129.3 (2 × d), 130.8 (s), 132.1 (s), 132.7 (d), 139.7 (s), 149.9 (s), 154.0 (s), 154.1 (s), 173.3 (s). MS (EI, 70 eV) *m*/*z* (rel intensity) 465 (M^+ − 1, 39), 361 (73), 213 (27), 186 (36), 121 (38), 119 (32), 105 (100), 77 (27). Anal. Calcd for $C_{27}H_{22}N_4O_2S$ (466.55): C, 69.51; H, 4.75; N, 12.01; S, 6.87. Found: C, 69.34; H, 4.80; N, 11.92; S, 6.95.

(5*R,10a*S**)-2,8-Diphenyl-5-[(1*R**)-1-phenylethyl]-5,10a-dihydrothiazolo[5,4-*c*][1,2,4]triazolo[1,2-*a*]pyridazin-7,9-dione (9a).** AcOEt/hexane (1:2) was used as eluent (R_f 0.33). Yield 31%; mp 112−114 °C (colorless prisms, $CHCl_3$/*n*-hexane); IR (nujol) 1774, 1714, 1541, 1501, 1409, 1260, 953, 761, 687 cm^{-1}; ^1H NMR ($CDCl_3$) δ 1.34 (d, 3H, J = 7.2 Hz), 3.91 (qd, 1H, J = 7.1 Hz, J = 4.7 Hz), 5.04 (dt, 1H, J = 4.7 Hz, J = 3.4 Hz), 5.87 (t, 1H, J = 3.1 Hz), 5.93 (t, 1H, J = 3.1 Hz), 7.27−7.31 (m, 1H), 7.35−7.42 (m, 5H), 7.45−7.51 (m, 4H), 7.53−7.57 (m, 3H), 7.90−7.92 (m, 2H); ^{13}C NMR ($CDCl_3$) δ 13.2 (q), 40.8 (d), 58.3 (d), 65.3 (d), 113.5 (d), 125.2 (2 × d), 127.2 (d), 128.0 (2 × d), 128.3 (2 × d), 128.4 (d), 128.7 (2 × d), 128.8 (2 × d), 129.2 (2 × d), 130.8 (s), 132.1 (s), 132.7 (d), 140.5 (s), 149.0 (s), 154.3 (s), 155.1 (s), 173.1 (s). MS (EI, 70 eV) *m*/*z* (rel intensity) 466 (M^+, 21), 464 (36), 376 (40), 361 (89), 316 (55), 215 (70), 121 (63), 119 (72), 105 (100), 103 (51), 91 (55), 77 (68). Anal. Calcd for $C_{27}H_{22}N_4O_2S$ (466.55): C, 69.51; H, 4.75; N, 12.01; S, 6.87. Found: C, 69.13; H, 4.88; N, 12.21; S, 6.99.

Synthesis of Compounds 10a and 11a. PTAD (0.02 g, 0.11 mmol) was added to a solution of **8a** or **9a** (0.05 g, 0.11 mmol) in toluene (5 mL). The reaction mixture was stirred at room temperature for 12 h. After removal of the solvent under reduced pressure, the residue was purified by silica gel column chromatography.

(4*R,5*R**)-2,8-Diphenyl-4-(4-phenyl-3,5-dioxo-1,2,4-triazolidin-1-yl)-5-[(1*S**)-1-phenylethyl]-4,5-dihydrothiazolo[5,4-*c*][1,2,4]-triazolo[1,2-*a*]pyridazin-7,9-dione (10a).** AcOEt/hexane (1:1) was used as eluent (R_f 0.37). Yield 92%; mp 164−166 °C (colorless

(52) Hudson, R. F.; Chopard, P. A. *J. Org. Chem.* **1963**, *28*, 2446−2447.

(53) Thiazole **7a** was obtained with minor impurities after purification by column chromatography. It was used for the next step without further purification. The NMR spectra shown in the Supporting Information were obtained from a first fraction obtained in a second chromatography.

prisms, $CHCl_3$/*n*-hexane); IR (nujol) 1767, 1724, 1700, 1502, 1434, 1291, 1149, 760, 687 cm^{-1}; ^1H NMR ($CDCl_3$) δ 1.37 (d, 3H, J = 7.0 Hz), 2.99 (dq, 1H, J = 10.5 Hz, J = 7.0 Hz), 5.03 (dd, 1H, J = 10.5 Hz, J = 0.9 Hz), 5.44 (d, 1H, J = 0.9 Hz), 7.17−7.20 (m, 2H), 7.27−7.47 (m, 16H), 7.80−7.83 (m, 2H), 8.52 (broad s, 1H, NH); ^{13}C NMR ($CDCl_3$) δ 19.2 (q), 42.0 (d), 52.3 (d), 61.5 (d), 125.5 (2 × d), 125.7 (2 × d), 126.3 (2 × d), 127.4 (2 × d), 127.9 (d), 128.2 (d), 128.6 (d), 129.06 (2 × d), 129.09 (2 × d), 129.25 (2 × d), 129.28 (2 × d), 129.8 (s), 129.9 (s), 130.4 (s), 130.50 (s), 130.52 (d), 132.5 (s), 140.2 (s), 146.7 (s), 149.4 (s), 151.4 (s), 153.4 (s), 161.9 (s). EM (FAB^+) *m*/*z* (%): 642 ($M^+ + 1$, 46). Anal. Calcd for $C_{35}H_{27}N_7O_4S$ (641.72): C, 65.51; H, 4.24; N, 15.28; S, 5.00. Found: C, 65.32; H, 4.32; N, 15.30; S, 5.11.

(4*R,5*R**)-2,8-Diphenyl-4-(4-phenyl-3,5-dioxo-1,2,4-triazolidin-1-yl)-5-[(1*R**)-1-phenylethyl]-4,5-dihydrothiazolo[5,4-*c*][1,2,4]triazolo[1,2-*a*]pyridazin-7,9-dione (11a).** AcOEt/hexane (1:1) was used as eluent (R_f 0.29). Yield 85%; mp 303−305 °C (colorless prisms, $CHCl_3$/*n*-hexane); IR (nujol) 1775, 1713, 1555, 1150, 873, 721 cm^{-1}; ^1H NMR ($CDCl_3$) δ 1.59 (d, 3H, J = 6.9 Hz), 2.91 (dq, 1H, J = 10.4 Hz, J = 6.9 Hz), 4.87 (dd, 1H, J = 10.4 Hz, J = 0.9 Hz), 5.95 (d, 1H, J = 0.9 Hz), 6.87−6.89 (m, 2H), 7.16−7.45 (m, 17H), 7.85−7.87 (m, 2H); ^{13}C NMR ($CDCl_3$) δ 18.9 (q), 41.8 (d), 53.7 (d), 62.5 (d), 125.4 (2 × d), 125.5 (2 × d), 126.2 (2 × d), 128.1 (d), 128.3 (2 × d), 128.37 (d), 128.44 (d), 128.6 (2 × d), 128.9 (2 × d), 129.1 (2 × d), 129.2 (2 × d), 129.4 (s), 129.6 (s), 130.0 (s), 130.61 (s), 130.64 (d), 132.4 (s), 139.5 (s), 146.0 (s), 148.4 (s), 152.3 (s), 153.4 (s), 162.0 (s). EM (FAB^+) *m*/*z* (%): 642 ($M^+ + 1$, 37). Anal. Calcd for $C_{35}H_{27}N_7O_4S$ (641.72): C, 65.51; H, 4.24; N, 15.28; S, 5.00. Found: C, 65.39; H, 4.35; N, 15.33; S, 5.07.

Acknowledgment. We are grateful to the "Ministerio de Educación y Ciencia" (MEC) of Spain and FEDER (Project CTQ2005-02323/BQU) as well to the "Fundación Séneca-CARM" (Project 00458/PI/04) for funding. J.C. is also grateful to the MEC for a fellowship. This work is warmly dedicated to Prof. Dr. Waldemar Adam on the occasion of his 70th birthday.

Supporting Information Available: Full characterization of compounds **2b**−**d**, **8b**,**c**, **9b**,**c**, α-chloroketones **7b**−**c**, and thiazoles **4b**,**c**; figure showing the X-ray crystal structure of **10a**; ^1H and ^{13}C NMR spectra for new compounds; Cartesian coordinates, electronic energies and low frequencies, relevant geometrical and electronic parameters (natural charges), and relative energies using the PCM-method of the local minima and transition structures discussed in the text; crystallographic information file (CIF) for **10a**. This material is available free of charge via the Internet at http://pubs.acs.org.

JO7021668